Liquid Crystals
Publication details, including instructions for authors and subscription information:
http://www.informaworld.com/smpp/title~content=t713926090

A dielectric study of three chiral liquid crystals presenting SmC^*_{FI} phases

S. Sarmento; P. Simeão Carvalho; M. R. Chaves; F. Pinto; H. T. Nguyen

Online publication date: 06 August 2010

To cite this Article Sarmento, S. , Carvalho, P. Simeão , Chaves, M. R. , Pinto, F. and Nguyen, H. T.(2001) 'A dielectric study of three chiral liquid crystals presenting SmC^*_{FI} phases', Liquid Crystals, 28: 5, 673 — 690
To link to this Article: DOI: 10.1080/02678290010028744
URL: http://dx.doi.org/10.1080/02678290010028744

LIQUID CRYSTALS, 2001, VOL. 28, NO. 5, 673–690

A dielectric study of three chiral liquid crystals presenting SmC^*_{FI} phases

S. SARMENTO, P. SIMEÃO CARVALHO, M. R. CHAVES*, F. PINTO
Departamento de Física, IMAT (Núcleo IFIMUP), CFUP,
Faculdade de Ciências da Universidade do Porto, Rua do Campo Alegre 687,
4169-007 Porto, Portugal

and H. T. NGUYEN
Centre de Recherche Paul Pascal, Av. A. Schweitzer, 33600 Pessac, France

(*Received 17 June 2000; in final form 28 October 2000; accepted 22 November 2000*)

We have performed a detailed dielectric study of three compounds presenting ferrielectric phases over large temperature intervals. The relaxation processes detected in the SmC^*_{FI} phases are highly polidispersive. We have repeatedly observed the surface layer mode described by Bourny *et al.* [1] and a weak ferrielectric mode, whose relaxation frequency is always higher on heating than on cooling runs. The temperature interval where SmC^*_{FI} phases occur is apparently independent of cooling/heating rates and of the history of the sample.

1. Introduction

The structure of the ferrielectric SmC^*_{FI} phases is presently a subject of debate. Recent X-ray results from freely suspended films [2] were interpreted on the basis of the clock model [3], and a periodicity of three and four layers was found for the $SmC^*_{FI_1}$ and $SmC^*_{FI_2}$ phases, respectively. The clock model was originally proposed to describe the behaviour of the SmC^*_α phase [3], but it is also compatible with a three- or four-layer periodicity in SmC^*_{FI} phases if flexoelectric terms are taken into account [4]. However, a structure with a constant phase difference between nearest layers of 90° ($SmC^*_{FI_2}$, four-layer periodicity) or 120° ($SmC^*_{FI_1}$, three-layer periodicity) is incompatible with some well known experimental results, obtained from conoscopy or optical rotatory power (ORP) measurements [5]. On the other hand, the so-called Ising model [6] explains the measurements obtained from optical rotatory power and conoscopy, but this model is incompatible with the X-ray results of Mach *et al.* [2]. Several atempts have been made to reconcile X-ray results with conoscopy and optical rotatory power data by considering distorted versions of the clock and Ising models. Akizuki *et al.* [5] have calculated the maximum distortion to the Ising model compatible with conoscopy results, but this requirement is apparently incompatible with the maximum possible distortion of the clock model permitted by X-ray results, as estimated by Cluzeau *et al.* [7].

Several authors have performed dielectric measurements on liquid crystal materials presenting antiferroelectric and ferrielectric phases [8–14]. Some investigations were mostly concerned with the relaxation processes of the SmC^*_A phase [8, 9, 12]. In the ferrielectric phases, Fukui *et al.* [13], Hou *et al.* [11], and Uehara *et al.* [14] observe a relaxation process whose dielectric contribution is high near the SmC*–SmC^*_γ phase transition and then decreases with decreasing temperature. The relaxation frequency of this process is approximately constant and similar to that of the Goldstone mode in the SmC* phase [13, 14], but decreases markedly with decreasing temperature [11]. This relaxation process has been designated 'Goldstone mode' [13, 14], but here we will avoid this designation in SmC^*_{FI} phases. We feel that the present discussion concerning the structure of these phases makes it difficult to define what a 'Goldstone mode' is. In ferrielectric phases, Uehara *et al.* [14] also observe two modes in the mHz range and a relaxation process around 100 Hz, with a strong dielectric contribution that decreases with applied bias field and decreasing sample thickness. They related this relaxation process to the fluctuation of the helical structure.

*Author for correspondence; e-mail: rachaves@fc.up.pt

Liquid Crystals ISSN 0267-8292 print/ISSN 1366-5855 online © 2001 Taylor & Francis Ltd
http://www.tandf.co.uk/journals
DOI: 10.1080/02678290010028744

In this work, we have made detailed dielectric measurements on three compounds that present ferrielectric phases over large temperature intervals (2–6 K). The compounds studied have the general chemical formula:

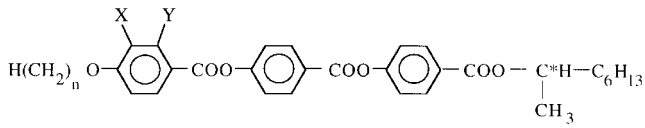

where for $n = 10$, $X = F$ and $Y = H$ and for $n = 11$, $X = F$ or H and $Y = H$.

Preliminary differential scanning calorimetry (DSC) measurements and texture observations have suggested the following phase sequences [15]†:

10FH

$$\mathrm{Cr} \underset{}{\overset{88.3\,^{\circ}\mathrm{C}}{\rightleftharpoons}} \mathrm{SmC}^*_{\mathrm{A}} \underset{101.8\,^{\circ}\mathrm{C}}{\rightleftharpoons} \mathrm{SmC}^*_{\mathrm{FI}} \underset{103.4\,^{\circ}\mathrm{C}}{\rightleftharpoons} \mathrm{SmC}^* \underset{112.8\,^{\circ}\mathrm{C}}{\rightleftharpoons}$$

$$\mathrm{SmC}^*_{\alpha} \underset{113.3\,^{\circ}\mathrm{C}}{\rightleftharpoons} \mathrm{SmA}^* \overset{127.1\,^{\circ}\mathrm{C}}{\rightleftharpoons} \mathrm{I}$$

11FH

$$\mathrm{Cr} \overset{82.0\,^{\circ}\mathrm{C}}{\rightleftharpoons} \mathrm{SmC}^*_{\mathrm{A}} \underset{85.2\,^{\circ}\mathrm{C}}{\rightleftharpoons} \mathrm{SmC}^*_{\mathrm{FI}} \underset{89.8\,^{\circ}\mathrm{C}}{\rightleftharpoons}$$

$$\mathrm{SmC}^* \underset{114.3\,^{\circ}\mathrm{C}}{\rightleftharpoons} \mathrm{SmA}^* \overset{124.6\,^{\circ}\mathrm{C}}{\rightleftharpoons} \mathrm{I}$$

11HH

$$\mathrm{Cr} \overset{82.5\,^{\circ}\mathrm{C}}{\rightleftharpoons} \mathrm{SmC}^*_{\mathrm{A}} \underset{86.2\,^{\circ}\mathrm{C}}{\rightleftharpoons} \mathrm{SmC}^*_{\mathrm{FI}_1} \underset{90.8\,^{\circ}\mathrm{C}}{\rightleftharpoons} \mathrm{SmC}^*_{\mathrm{FI}_2} \underset{92.7\,^{\circ}\mathrm{C}}{\rightleftharpoons}$$

$$\mathrm{SmC}^* \underset{117.4\,^{\circ}\mathrm{C}}{\rightleftharpoons} \mathrm{SmA}^* \overset{131.4\,^{\circ}\mathrm{C}}{\rightleftharpoons} \mathrm{I}$$

Previous Raman diffusion measurements on compound **10FH** show a clear change of behaviour in the middle of the ferrielectric region [16]. The ratios $R_1 = I_{yz}/I_{zz}$ and $R_2 = I_{zy}/I_{yy}$ exhibit a well defined two-step behaviour, with a clear change of slope in this temperature interval. This suggests that the ferrielectric region corresponds to two ferrielectric phases ($\mathrm{SmC}^*_{\mathrm{FI}_1}$ and $\mathrm{SmC}^*_{\mathrm{FI}_2}$), although the transition between them was not detected by DSC.

2. Experimental

The liquid crystals were filled by capillarity into commercial cells (E. H. C. Co, Japan), coated with ITO electrodes and rubbed polyimide. All measurements were made on planar, 25 μm thick samples.

The samples were placed in a specially built oven and the temperature was controlled with a Lakeshore DRC-93CA temperature controller, using a chromel-alumel thermocouple as a thermometer. The accuracy was about 0.05 K.

The dielectric constant was measured at stabilized temperatures on cooling and heating, in the frequency range 20 Hz–1 MHz, using a HP4284A LCR meter and a measuring a.c. electric field of 0.01 V μm^{-1}. The resistance of the electrodes in series with the liquid crystal sample mimics a false relaxation mode (ITO effect) around 1 MHz [17].

The following expression was fitted to the dielectric data:

$$\varepsilon^*(\omega) = \varepsilon(\infty) + \sum_j \frac{\Delta\varepsilon_j}{1 + \left(\mathrm{i}\frac{f}{f_{\mathrm{R}_j}}\right)^{\beta_j}} + \frac{1}{(\mathrm{i}\omega\tau_{\mathrm{c}})^{\gamma}} \qquad (1)$$

where $\Delta\varepsilon_j$, f_{R_j} and β_j are, respectively, the dielectric amplitude, relaxation frequency and dispersion parameter of the j-th mode. The third term in expression (1) accounts for the ionic conductivity, γ expressing the dispersion of 'conduction times' [13].

The helical pitch was measured by a diffraction method. Low frequency (0.1–2 Hz) optical hysteresis loops were obtained using a HP33120A signal generator and a Kepko (Bop 1000M) signal amplifier. The intensity of the transmitted light was measured with a BPW21 (R.S. components, Ltd) photodiode.

3. Experimental results and discussion

For the three compounds studied, the polar character of each phase was confirmed by optical hysteresis loops. Figure 1 shows some examples of optical hysteresis loops obtained in the temperature regions of the $\mathrm{SmC}^*_{\mathrm{FI}}$ phases of the three compounds studied. The optical hysteresis loop obtained in the antiferroelectric $\mathrm{SmC}^*_{\mathrm{A}}$ phase of **10FH** is also presented for comparison, as it shows a completely different optical behaviour. It can be seen that the loops of the $\mathrm{SmC}^*_{\mathrm{FI}}$ phases are characteristic of phases presenting ferrielectric-like behaviour [18]. On the other hand, there is no significant difference between the loops obtained in the $\mathrm{SmC}^*_{\mathrm{FI}_1}$ and $\mathrm{SmC}^*_{\mathrm{FI}_2}$ phases of **11HH**, although these two phases could be distinguished by DSC.

Having thus established the ferrielectric character of the $\mathrm{SmC}^*_{\mathrm{FI}}$ phases under study, we will now present and discuss the results obtained from dielectric measurements. First, each compound will be discussed separately in the three following subsections. The following two subsections deal with results obtained with different cooling/heating rates and under an applied bias field. Finally we will present a summary of the most important results obtained for all the compounds.

†The critical temperatures indicated were determined in heating runs (⇀) or cooling runs (↼).

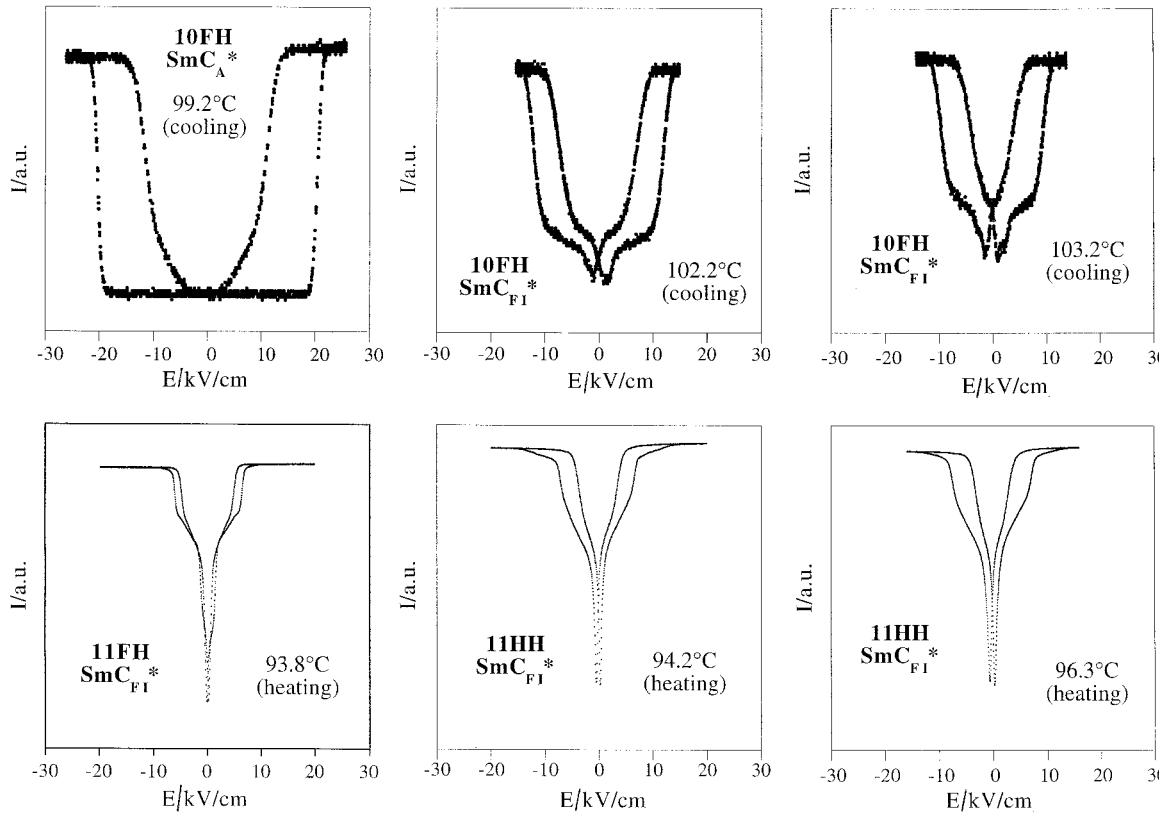

Figure 1. Typical optical hysteresis loops, obtained in the SmC_A^* and SmC_{FI}^* phases of **10FH** and in the SmC_{FI}^* phases of **11FH** and **11HH**.

3.1. *The compound **10FH***

Figure 2 summarizes the results obtained from fitting expression (1) to the dielectric data obtained on cooling, for the compound **10FH**. The parameters f_R, $\Delta\varepsilon$ and β for the different modes are presented as a function of temperature, respectively, in figures 2(*a*), 2(*b*) and 2(*c*). The dotted lines indicate the phase transition temperatures, as determined by several techniques [16].

In the SmA* phase, only the soft mode was detected. Its Curie–Weiss behaviour near the SmA*–SmC_α^* transition is shown in the insets of figures 2(*a*) and 2(*b*).

The relaxation frequency (f_R) and the dielectric amplitude ($\Delta\varepsilon$) present no anomalies across the SmA*–SmC_α^* and SmC_α^*–SmC* phase transitions, yet the value of the β parameter is lower in the temperature range of the SmC_α^* phase than in the neighbouring SmA* and SmC* phases, see figure 2(*c*). In the SmC_α^* phase, the soft mode is expected to coexist with the Goldstone mode, whose behaviour is usually described by the relations [19]:

$$\Delta\varepsilon_G = \frac{1}{4\pi\varepsilon_o}\frac{p^2}{2\pi K}\left(\frac{\mathbf{P}_o}{\theta_o}\right)$$
$$f_{R_G} = \frac{2\pi K}{p^2\gamma} \qquad (2)$$

where p is the helical pitch, and $\Delta\varepsilon_G$ and f_{R_G} are the dielectric amplitude and relaxation frequency of the Goldstone mode, respectively. $\mathbf{P}_o$ and θ_o are the spontaneous polarization and tilt angle, K is an elastic constant and γ a viscosity coefficient.

As the pitch in the SmC_α^* phase is very short [2, 20], the frequency of the Goldstone mode is high, of the same order as the frequency of the soft mode. Therefore, it may be impossible to distinguish the two modes in this phase [21].

The Goldstone mode is observed over the whole temperature range of the SmC* phase. Its dielectric amplitude presents a maximum ($\approx$220) at 112.6°C, then decreases to $\approx$160 at 108°C and increases again near the transition to the SmC_{FI}^* phase. The relaxation frequency shows, approximately, the inverse behaviour, with a minimum value of $\approx$1.7 kHz at 112.6°C and a maximum of $\approx$2.4 kHz at 108°C.

The dielectric relaxation processes of the SmC_A^* phase are not as well understood as those of the SmC* phase. Without applying a d.c. bias field, two relaxation processes are usually referred to in the literature [8–10], one in the kHz range and the other at higher frequency, below 1 MHz, denoted P_L and P_H, respectively [8]. There seems to exist a general agreement that the P_H

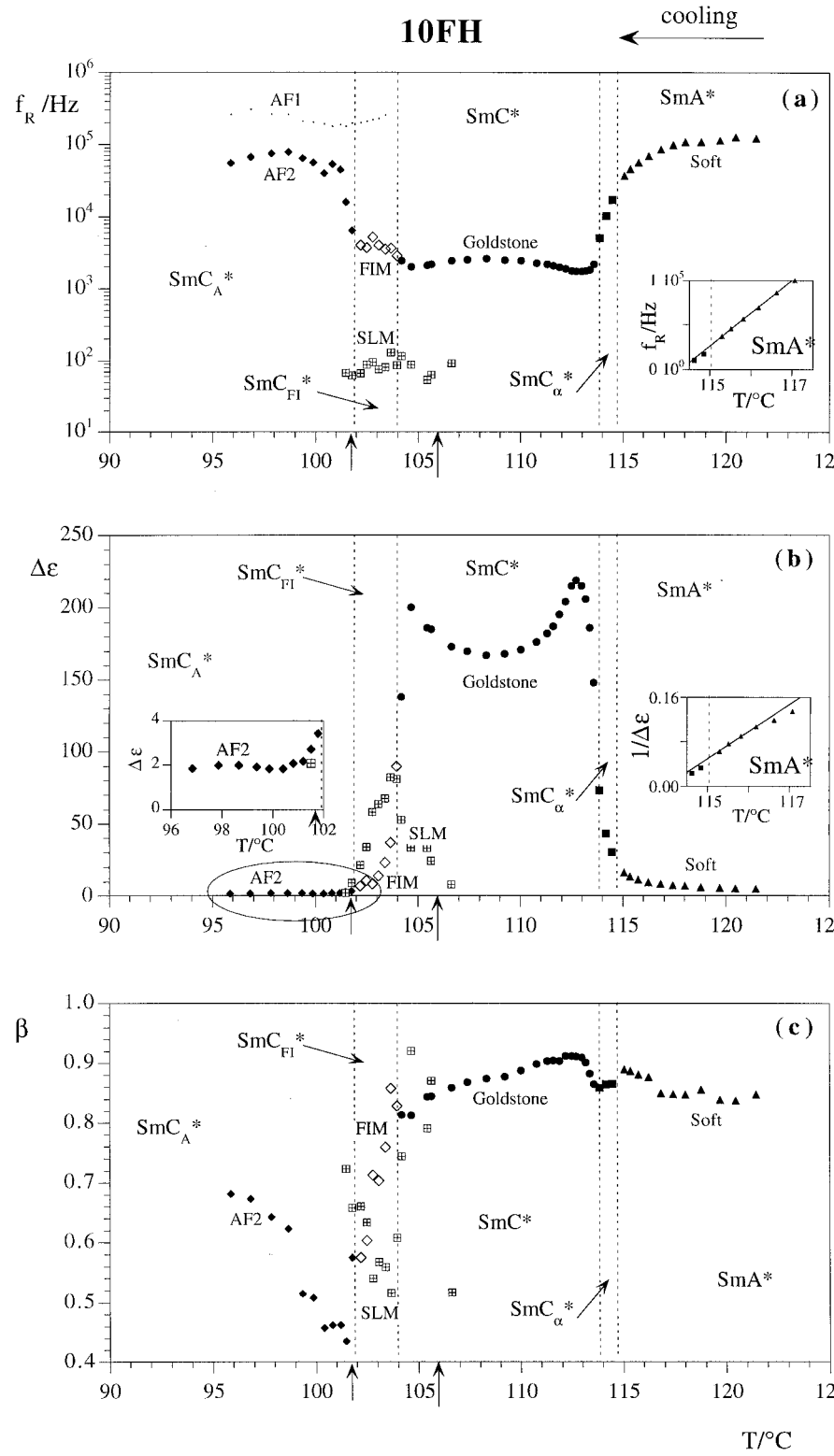

Figure 2. Relaxation frequencies (*a*), dielectric amplitudes (*b*) and dispersion parameters (*c*) of the relaxation modes detected for **10FH**, on cooling. The parameters were obtained from the fitting of equation (1) to the dielectric data obtained at stabilized temperatures.

mode corresponds to antiphase collective azimuthal motions of the molecules. As for the P_L mode, several attempts have been made to identify its nature. In [9] and [10] it has been attributed to a non-collective molecular rotation around the short axis, while in Buyvidas *et al.* [8] it corresponds to the in-phase collective azimuthal motion of the molecules. According to these authors, the helicoidal superstructure in the

SmC^*_A phase leads to an incomplete cancellation of the polarization in adjacent layers, so that this in-phase motion of the molecules may give a dielectric contribution.

In the SmC^*_A phase of **10FH** we also observe two relaxation modes, denoted AF1 and AF2 in figure 2. AF1 is a weak relaxation process at high frequency ($\approx$200 kHz) that was already present in the ferrielectric phase. It is impossible to characterize it accurately due to the ITO effect. A lower frequency mode, AF2, is also observed between 5 and 50 kHz. Its relaxation frequency increases sharply on cooling below the SmC^*_{FI}–SmC^*_A phase transition, then remains approximately constant around 50 kHz. We also observe that the dielectric amplitude and the relaxation frequency of this mode increase with an applied bias field. Therefore, it seems that the AF2 mode is related to some azimuthal movement of the molecules.

Our data are insufficient to identify the AF1 and AF2 modes beyond doubt with either P_L or P_H of reference [8]. However, taking into account the temperature behaviour of the relaxation frequency, it is plausible that the AF2 mode is the P_H mode of [8–10].

In the ferrielectric region we observe the weak AF1 mode and two other relaxation processes. One is observed both in the ferrielectric phase and in the low temperature region of the SmC* phase. Its relaxation frequency is around 100 Hz. This relaxation process is apparently related to the existence of visible disclination lines. It will be designated SLM (surface layer mode), following Bourny *et al.* [1]. A detailed description of this relaxation process and its relation to disclination lines is given in the next three subsections.

The other mode observed in the ferrielectric region has almost the same relaxation frequency as the Goldstone mode in the SmC* phase, but a much lower dielectric amplitude. We suggest that this mode is also due to some azimuthal reorientation of the molecules, and therefore closely related to the structure of the SmC^*_{FI} phase. In the present work it will be denoted ferrielectric mode (FIM).

3.1.1. *Disclination lines*

The helicoidal structure of the bulk SmC* phase is incompatible with planar anchoring at the surfaces. Usually, this leads to a regular structure of defects (2π disclinations), that can be easily observed by polarizing optical microscopy. However, in the SmC* phase of **10FH**, 2π-disclinations are not seen above $\approx$106°C, figure 3 (*a*) unless a d.c. electric field is applied, figure 3 (*b*). On cooling the sample below 106°C, the lines start to appear, figure 3 (*c*). Their contrast and density increase on further cooling, figure 3 (*d*), until the transition into the ferrielectric phase takes place.

One of the reasons why 2π-disclinations may not be seen is the very small pitch; another is the spontaneous unwinding of the helix. Neither of these conditions is consistent with the regular behaviour of the Goldstone mode around 106°C (see figure 2), nor with the regular temperature behaviour of the helical pitch obtained by a direct measurement (see figure 4).

Another possible explanation for the absence of disclination lines is the one suggested by Pavel *et al.* [22]. In the SmC* phase of materials presenting the SmC^*_A phase at lower temperatures, antiparallel defects on the surfaces (π-disclinations) may be energetically more favourable than 2π-disclinations in the bulk. As π-disclinations have very low optical contrast, they would not be seen. The applied d.c. electric field transforms pairs of π-disclinations into 2π-disclinations, which are visible by polarizing optical microscopy (POM).

3.1.2. *The surface layer mode in C8 tolane*

The antiferroelectric liquid crystals C8 and C10 tolane studied by Bourny *et al.* [1] presented visible disclination lines only in a limited temperature interval, corresponding to the low temperature part of the SmC* phase (both on heating and cooling runs, for C8; only on heating, for C10). Whenever these disclination lines were visible, a low frequency (0.1–1 kHz) relaxation process was detected, both by dielectric and electro-optical measurements. Its dielectric amplitude was of the same order as that of the Goldstone mode and increased with increasing density of lines. As 2π-disclinations are charged defects (while π-disclinations are not charged) [22], this relaxation process was attributed to the movement of 2π disclinations and designated SLM (surface layer mode) [1].

3.1.3. *The surface layer mode in **10FH***

The small arrows in figure 2 indicate the limits of the temperature interval where disclination lines can be seen without a bias field. Throughout this temperature interval, we detect a polydispersive mode of approximately constant frequency ($\approx$100 Hz). Its dielectric contribution has a maximum at the SmC*–SmC^*_{FI} phase transition. A relaxation process with similar characteristics was also detected for **11FH** and **11HH** (as we shall discuss later), whenever disclination lines were visible. The dielectric amplitude of the mode appears to be strongly correlated to the density of lines observed. Therefore, we ascribe this low-frequency relaxation mode to the 'surface layer mode' described by Bourny *et al.* [1].

In **10FH** the SLM is largely responsible for the step observed in the dielectric measurements, in the temperature interval corresponding to the SmC^*_{FI} phase (see figure 5). In this region, the dielectric amplitude of

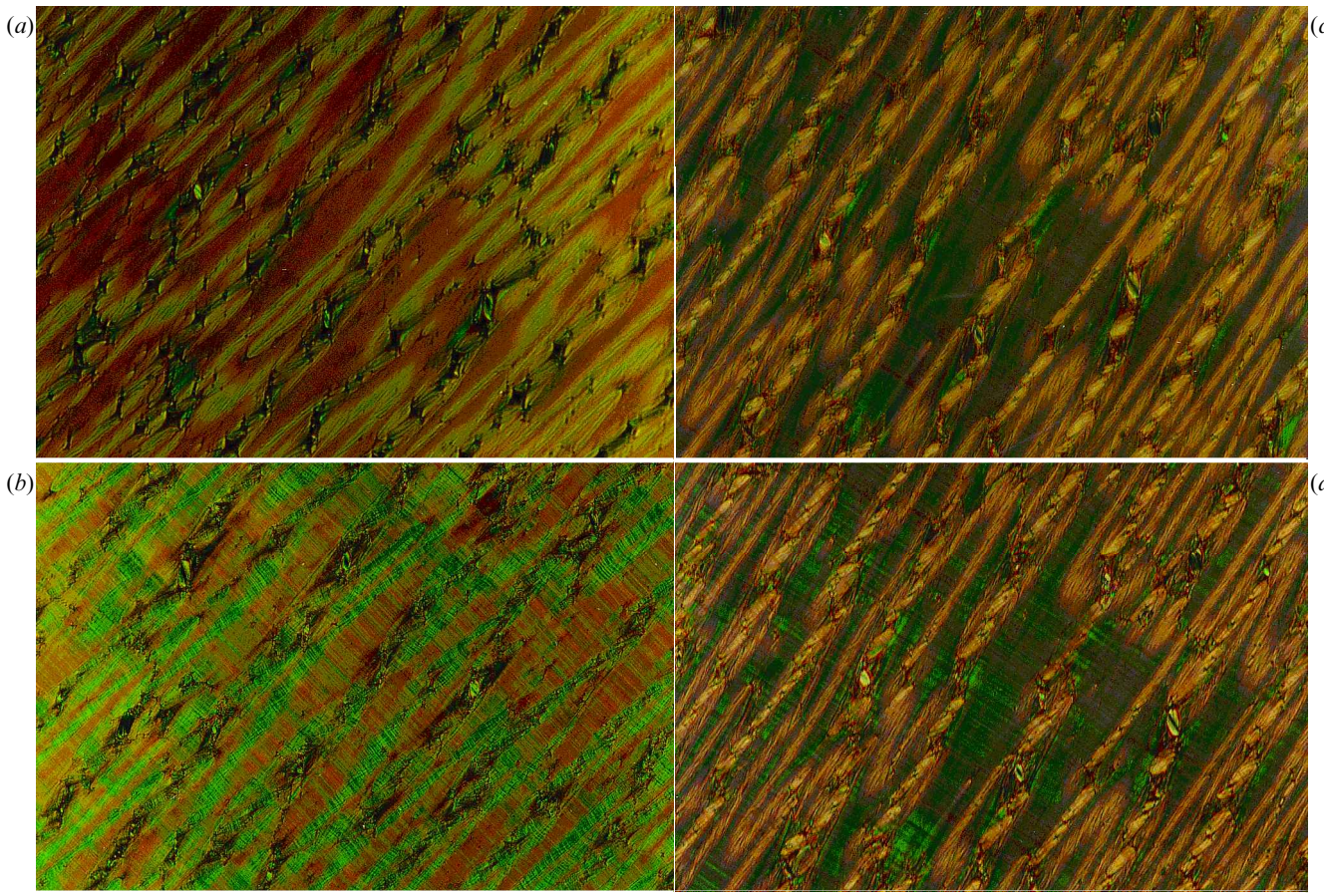

Figure 3. (*a*) The SmC* phase of compound **10FH** at 109°C on cooling, with $V_{d.c.} = 0$ V. Disclination lines are not visible. (*b*) The SmC* phase of compound **10FH** at 109°C on cooling, with $V_{d.c.} = 3.5$ V (sample thickness = 25 μm). Under the applied d.c. electric field, disclination lines become visible. (*c*) The SmC* phase of compound **10FH** at 106°C on cooling, with $V_{d.c.} = 0$ V. Disclination lines start to appear, but their contrast is still very low. (*d*) The SmC* phase of compound **10FH** at 104.7°C on cooling, with $V_{d.c.} = 0$ V. Disclination lines are now clearly observed.

the FIM is very weak and increases continuously, without noticeable steps as the temperature increases, see figure 2 (*b*).

3.1.4. *Dielectric relaxation of **10FH** on heating*

Figure 6 summarizes the results obtained from fitting the expression (1) to the dielectric data obtained on heating, for the compound **10FH**. The parameters f_R, $\Delta\varepsilon$ and β for the different modes are presented as a function of temperature, respectively in figures 6 (*a*), 6 (*b*) and 6 (*c*).

In the SmC^*_{FI} phase, we observe that the relaxation frequency of the FIM on heating, is higher than on cooling. This behaviour of the FIM is also observed for the other compounds studied, **11FH** and **11HH**.

In the SmC* phase, the dielectric contribution of the Goldstone mode is over 170 on cooling, and around a third of this value (≈ 50) on heating. Moreover, its relaxation frequency on heating (≈ 4 kHz) is approximately twice as much as on cooling (≈ 2 kHz). In the SmC^*_A phase, the low frequency X-mode was found only on heating. Both the unusual behaviour of the Goldstone mode and the presence of the X-mode were found only for this compound and will be discussed elsewhere [23].

3.2. *The compound **11FH***

All the dielectric relaxation modes detected for **10FH** on cooling were also observed for **11FH**. However, although the presence of the AF1 mode was detected in the SmC^*_A and SmC^*_{FI} phases of **11FH** around 1 MHz, it was impossible to extract any information on this mode from the fitting of equation (1), due to the ITO effect. The relaxation frequencies, dielectric amplitudes and relaxation parameters of the other modes are presented in figures 7 (cooling) and 8 (heating) as functions of temperature. The dotted lines indicate the phase transition temperatures, as determined from optical observations of the texture, dielectric and DSC measurements, hysteresis loops and TSM [24].

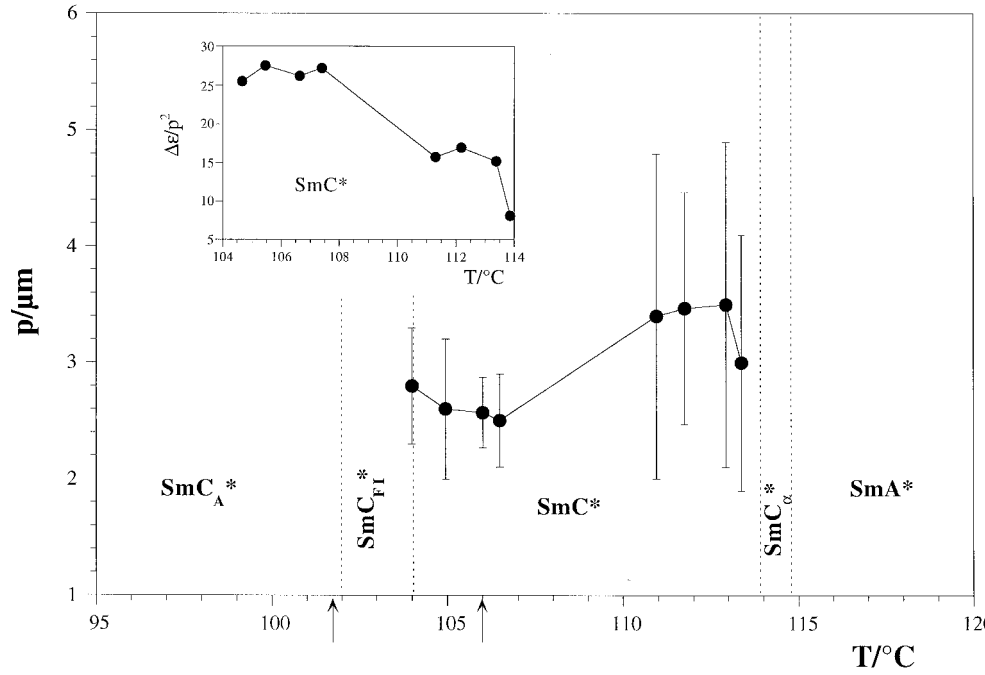

Figure 4. The helical pitch as a function of temperature, on cooling, for **10FH**. The values of p were obtained by a diffraction method. The inset shows the ratio $\Delta\varepsilon/p^2$ as a function of temperature

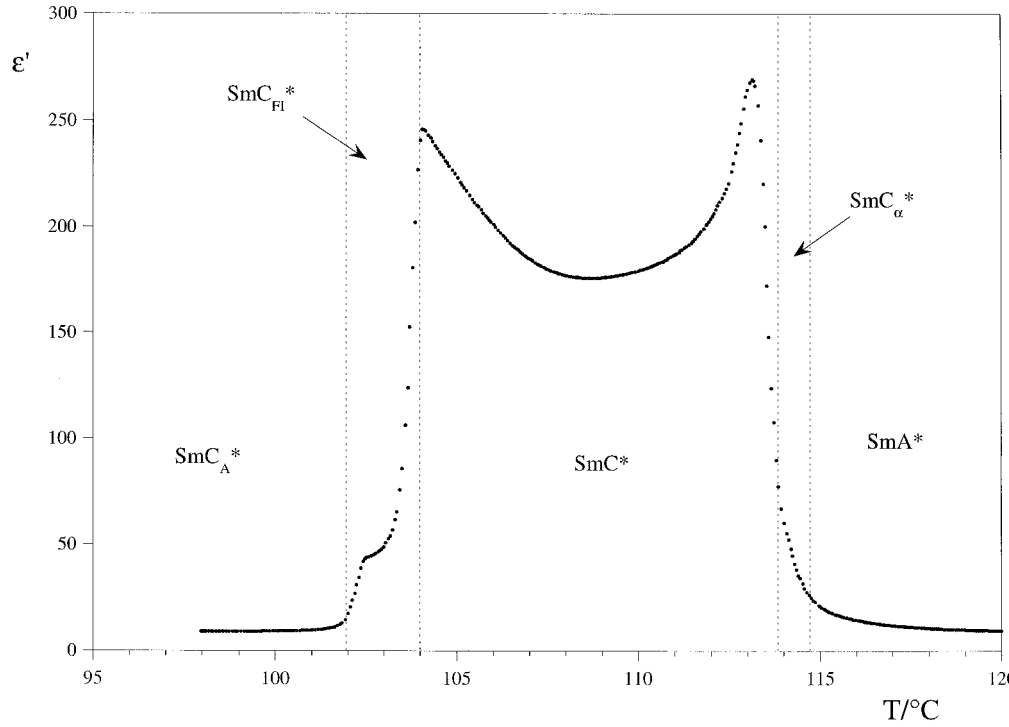

Figure 5. The real part of the dielectric constant, obtained at 100 Hz on cooling, for **10FH**.

The soft mode is detected at the beginning of the SmA* phase, but its relaxation frequency quickly rises beyond the measuring range of our experimental set-up.

In the SmC* phase below ≈112.5°C, the Goldstone mode presents a relaxation frequency of ≈4 kHz and a dielectric amplitude of ≈40, both on cooling and on

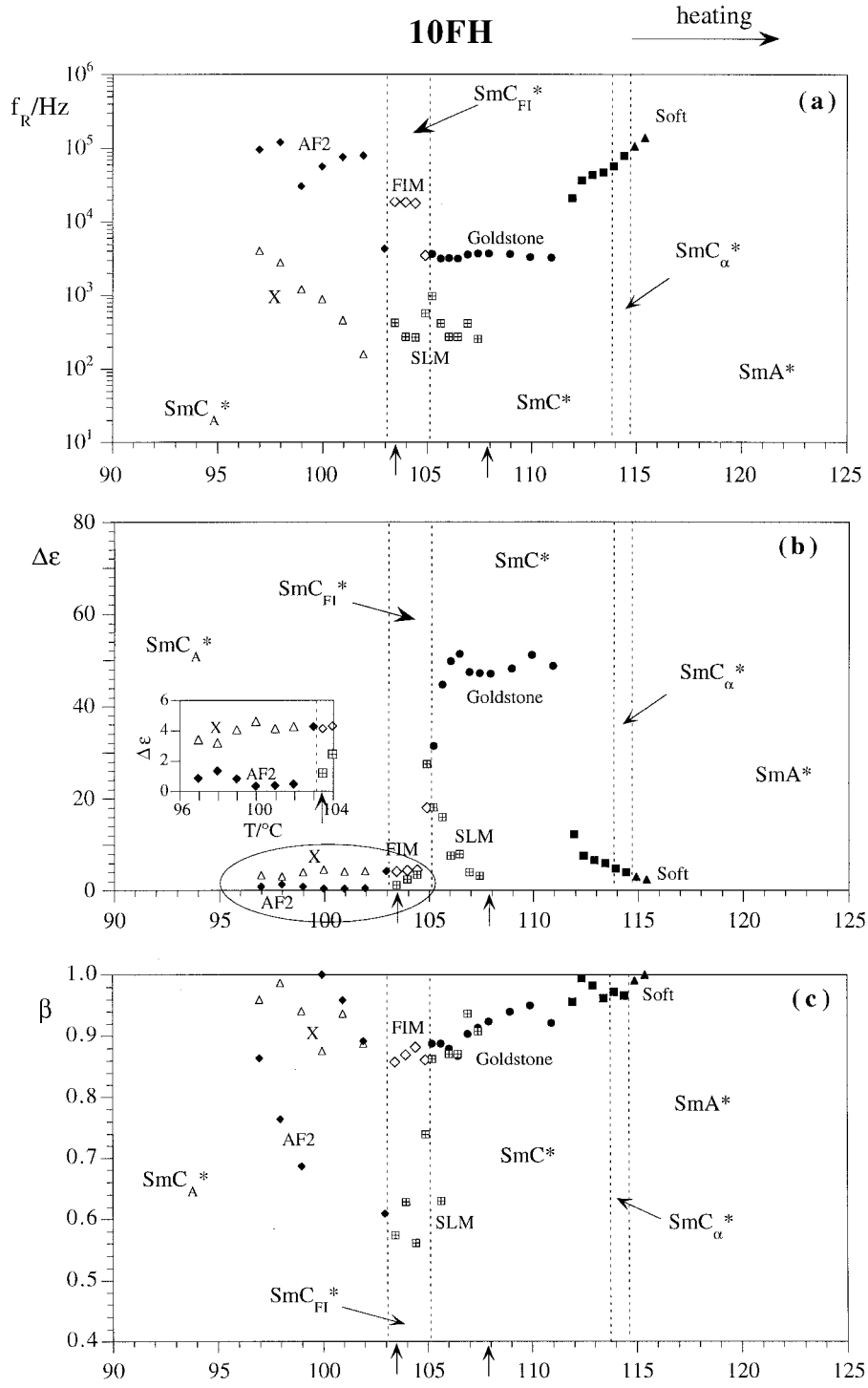

Figure 6. Relaxation frequencies (*a*), dielectric amplitudes (*b*) and dispersion parameters (*c*) of the relaxation modes detected for **10FH**, on heating.

heating (see figures 7 and 8). On heating, the dispersion parameter β is less than 0.9 at the SmC^*_{FI}–SmC* phase transition. Then it increases and remains constant at $\approx$0.95, indicating an almost monodispersive mode, see figure 7 (*c*).

Between $\approx$112.5°C and the transition to the SmA* phase at $\approx$115.2°C, the dielectric amplitude of the Goldstone mode decreases and its relaxation frequency increases. In fact, the relaxation process observed in this temperature interval is probably a mixture of the Goldstone mode with the soft mode, so that the softening of the latter is not observed.

The DSC measurements did not detect the presence of a SmC^*_α phase for this compound. Moreover, the

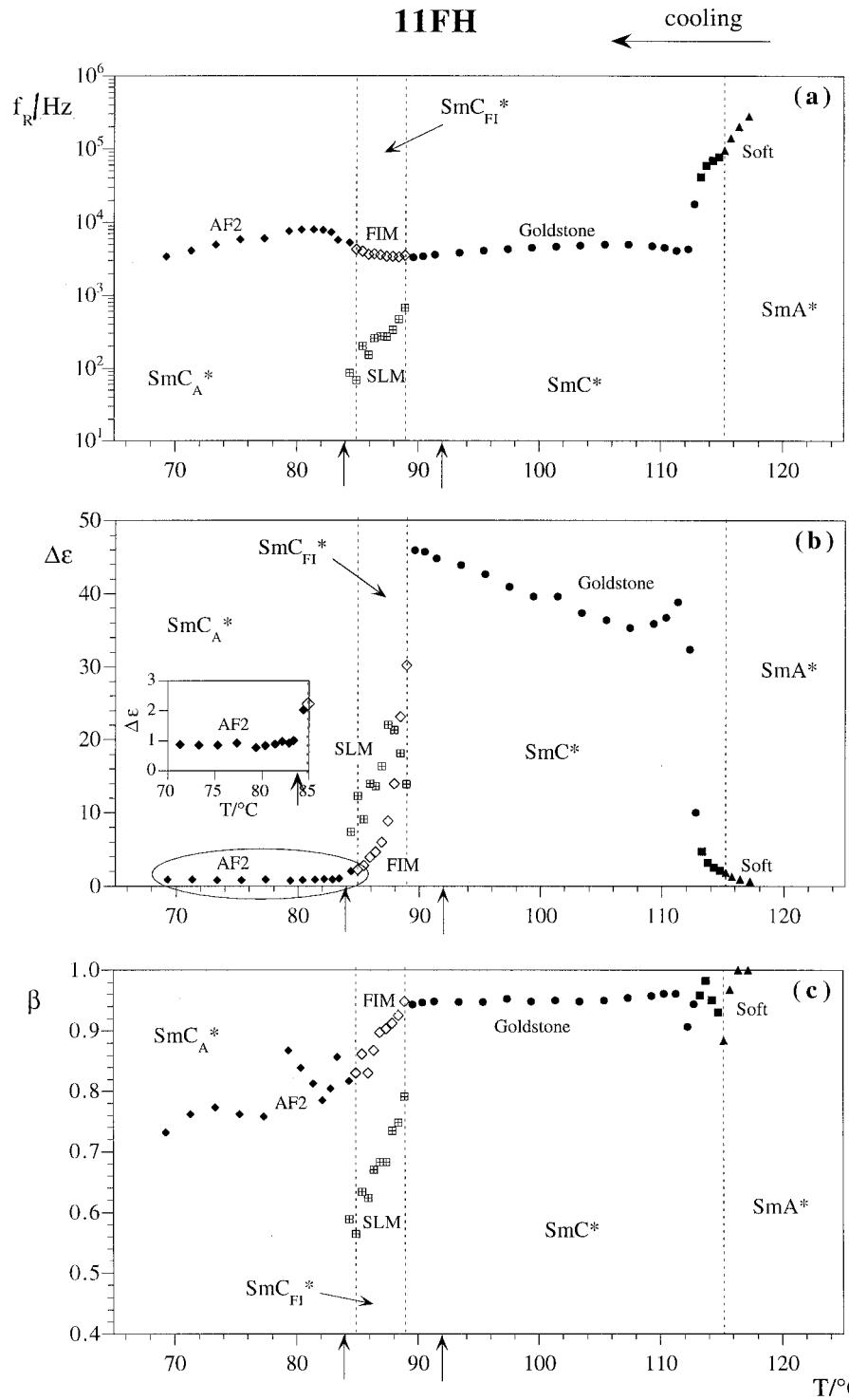

Figure 7. Relaxation frequencies (*a*), dielectric amplitudes (*b*) and dispersion parameters (*c*) of the relaxation modes detected for **11FH**, on cooling.

optical hysteresis loops obtained in this temperature range are not characteristic of the SmC^*_α phase [18, 25]. On the other hand, a decrease in the value of the helical pitch in the SmC* phase would result in a Goldstone mode with high frequency and low dielectric amplitude, see relations (2). According to [22], the interaction between π-disclinations of the same sign decreases the elastic energy. We suggest that this interaction promotes the structure with a small helical pitch in the high temperature part of the SmC* phase.

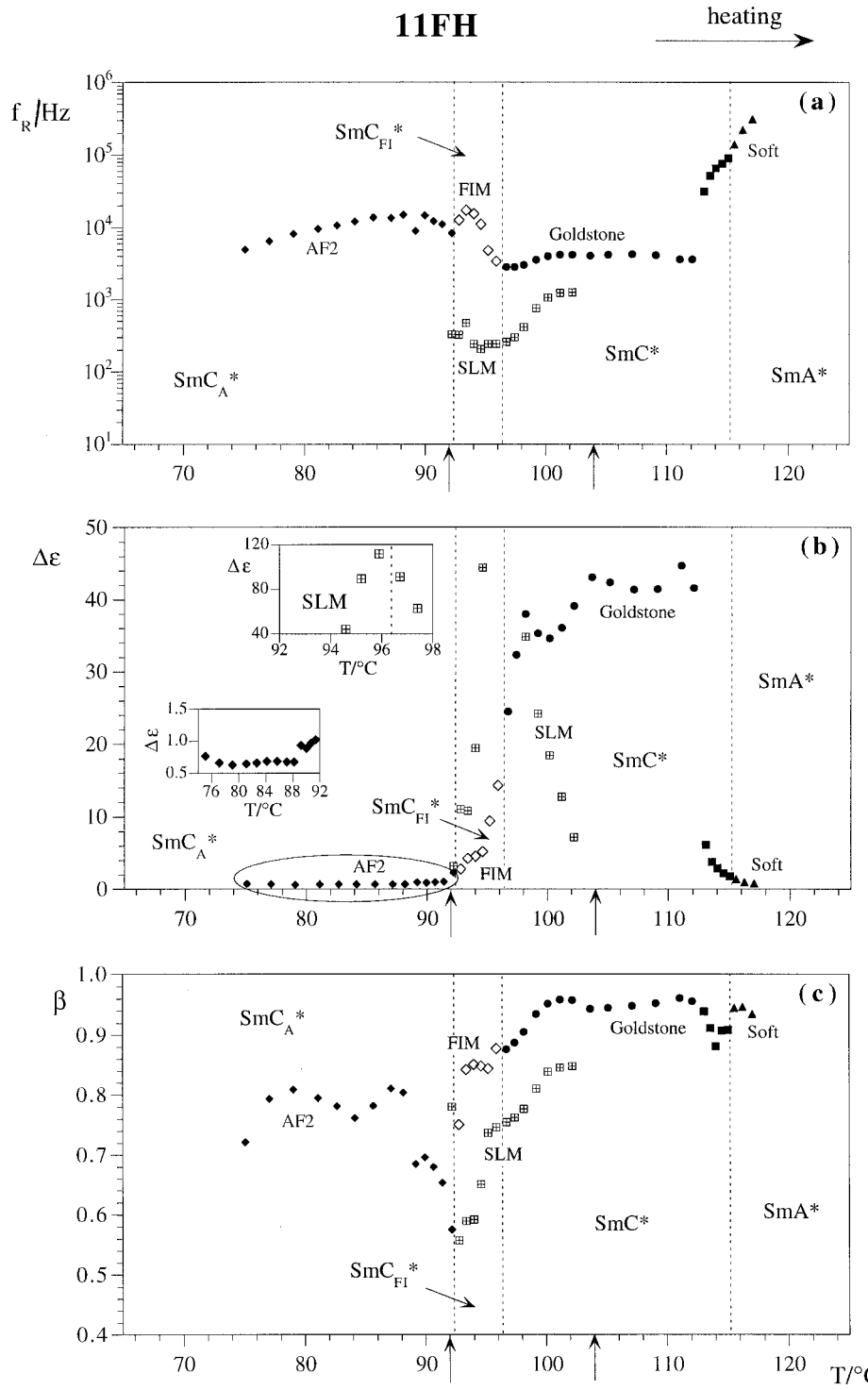

Figure 8. Relaxation frequencies (*a*), dielectric amplitudes (*b*) and dispersion parameters (*c*) of the relaxation modes detected for **11FH**, on heating.

The small arrows in figures 7 and 8 indicate the temperature interval where disclination lines could be observed by POM. The surface layer mode was detected inside this temperature interval, with a relaxation frequency between 100 Hz and 1 kHz. Its dielectric amplitude is much higher on heating than on cooling. This is in good agreement with the greater density of lines observed on heating. The maximum dielectric amplitude of the SLM occurs approximately at the temperature of the SmC*–SmC^*_{FI} phase transition.

The FIM was observed throughout the SmC^*_{FI} phase. Its relaxation frequency is higher on heating than on cooling, as already observed for **10FH**.

In the SmC^*_A phase of **11FH**, the AF2 mode presents similar characteristics on cooling and on heating: $\beta \approx 0.7$–0.8, $f_R \approx 5$–8 kHz. The relaxation frequency range of AF2 is similar to that of the Goldstone mode in the SmC* phase.

3.3. *The compound **11HH***

The dielectric relaxation study of **11HH** revealed several different modes. The corresponding relaxation frequencies, dielectric amplitudes and dispersion parameters are presented, as functions of temperature, in figures 9 (cooling) and 10 (heating). The dotted lines indicate the phase transition temperatures, as determined from optical observations of the texture, dielectric and DSC measurements, hysteresis loops and TSM [24].

All the six relaxation modes detected for **11FH** were also observed for **11HH**. Mode Z and mode Y were detected only for **11HH**. Mode Z presents a relaxation frequency around 1 kHz and is detected even in the SmA* phase. It is probably due to ionic charges in the sample. Mode Y is observed in most of the SmC* phase range, with a relaxation frequency of ≈ 100 kHz and a dielectric amplitude of ≈ 2. Its relaxation frequency is too low for it to be identified with the soft mode, which is detected in the SmA* phase. The temperature behaviour of the Y mode resembles that of the so-called triggered mode observed by Carvalho *et al.* [18] in a compound presenting the SmC^*_α phase.

Although the presence of the SmC^*_α phase was not detected by DSC for **11HH**, the relaxation frequency of the Goldstone mode increases sharply at ≈ 114°C, and its dielectric amplitude decreases. Between 114°C and the transition to the SmA* phase, at 117.4°C, only one relaxation process is observed, which is probably a superposition of the Goldstone and Y modes. This could be due to a decrease of the helical pitch, as already discussed for **11FH**. However, for **11HH**, the shape of the optical hysteresis loops obtained in this temperature interval, together with the presence of the Y mode, suggest the existence of the SmC^*_α phase. As pointed out by Žekš [26], if the SmC^*_α–SmC* phase transition is second order, the SmC^*_α phase should be experimentally indistinguishable from a SmC* phase with a small pitch. In fact, in the SmC* phase below 114°C, the Goldstone mode gives a relaxation frequency around 7 kHz and a dielectric amplitude of ≈ 17. The weak dielectric amplitude and high relaxation frequency suggest a small helical pitch.

11HH presents visible disclination lines over a large temperature interval. On cooling, they can be seen throughout most of the SmC* phase, in the ferrielectric region and nearly four degrees into the SmC^*_A phase. On heating, the lines appear only at 96°C, but their density is much higher than on cooling. Their number is a maximum at the SmC^*_{FI}–SmC* phase transition, then decreases on further heating until at ≈ 114°C they can no longer be seen. The SLM is detected throughout the temperature intervals where disclination lines are visible.

The dielectric spectrum of **11HH** is clearly much more complex than that of **10FH** or **11FH**. The presence of the Z mode suggests a large number of ionic impurities. The presence of 2π-disclinations and of the SLM over a large temperature interval suggests a peculiar surface anchoring. As similar cells were used for the three compounds, this difference is probably related to different interactions between the molecules and the substrate. Finally, it is possible that in **10FH** and **11FH**, the relatively high dielectric contribution of the Goldstone mode masks weaker contributions from other modes.

3.4. *Influence of cooling/heating rates*

Figures 11 and 12 show the real part of the dielectric constant, measured at 100 Hz, as a function of temperature for different cooling/heating rates, respectively, for **11HH** and **11FH**. Comparing figure 11 with figures 9 (*b*) and 10 (*b*), we see that the behaviour of ε' in the ferrielectric region of **11HH** is largely determined by the contributions of the SLM and mode Z. The behaviour of these two modes depends somewhat on cooling/heating rates and on the history of the sample. However, the size of the temperature intervals corresponding to the $SmC^*_{FI_1}$ and $SmC^*_{FI_2}$ phases is independent of cooling/heating rates.

Similarly, for **11FH** the behaviour of ε' in the SmC^*_{FI} phase is mostly due to the SLM, as can be seen by comparing figure 12 with figures 7 (*b*) and 8 (*b*). Again, we find that different cooling/heating rates do not influence the temperature interval where the SmC^*_{FI} phase occurs, for **11FH** (see figure 12).

Also important is that the dielectric characteristics of these phases are stable over large periods of time. Figure 13 shows two dielectric dispersion curves, obtained in the $SmC^*_{FI_1}$ phase of **11HH** at the same stabilized temperature (≈ 95.3°C on heating). The two curves were obtained with an interval of 5 h. No differences are observed except small fluctuations within experimental error.

A similar result was obtained in the SmC^*_{FI} phase of **11FH**: the dielectric dispersion curve was found to be stable, within experimental error, over an interval of 6 h.

3.5. *Measurements under a bias field*

Measurements with an applied bias field were performed only on **11FH**. This compound was chosen because its dielectric spectrum is simpler than that of **11HH**.

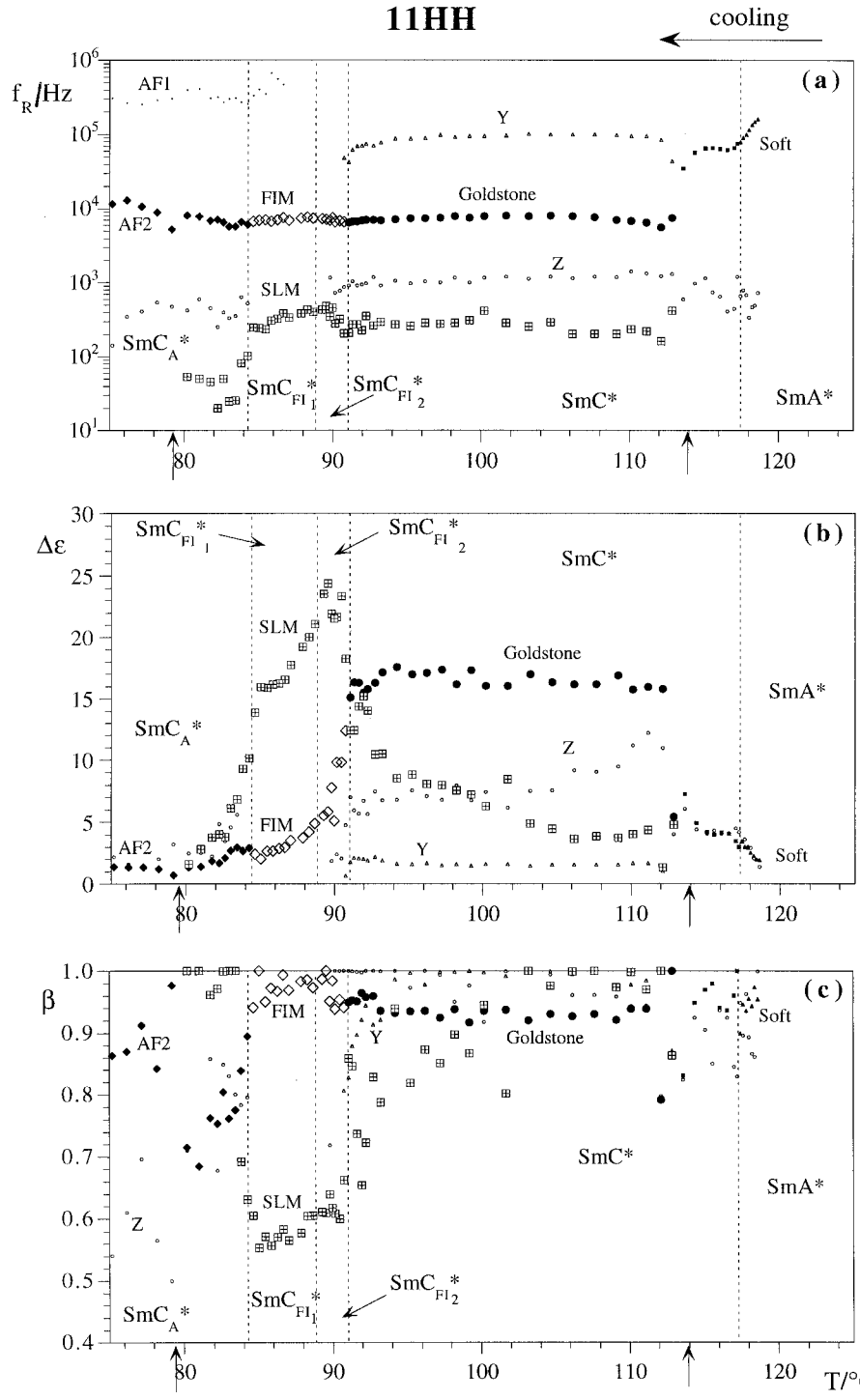

Figure 9. Relaxation frequencies (*a*), dielectric amplitudes (*b*) and dispersion parameters (*c*) of the relaxation modes detected for **11HH**, on cooling.

Moreover, **11FH** does not present hysteresis effects like those found for **10FH** [23]. In the SmC* phase of **11FH** on cooling, the lines become visible for $\mathbf{E}_{d.c.} = 0$ V μm^{-1} at ≈92°C. Below this temperature and until the transition to the SmC^*_{FI} phase at ≈89°C, a bias field as low as ≈0.2 V μm^{-1} already makes the density of lines decrease. In the high temperature part of the SmC* phase (between 100 and 112°C), the lines become visible for $\mathbf{E}_{d.c.} \approx 0.3$ V μm^{-1}. We have measured the dielectric constant at 100 Hz, on cooling and heating runs, applying different values of bias electric field. The results are shown in figure 14. The dotted lines and the arrows indicate, respectively, phase transitions and the appearance of disclination lines, at $\mathbf{E}_{d.c.} = 0$ V μm^{-1}.

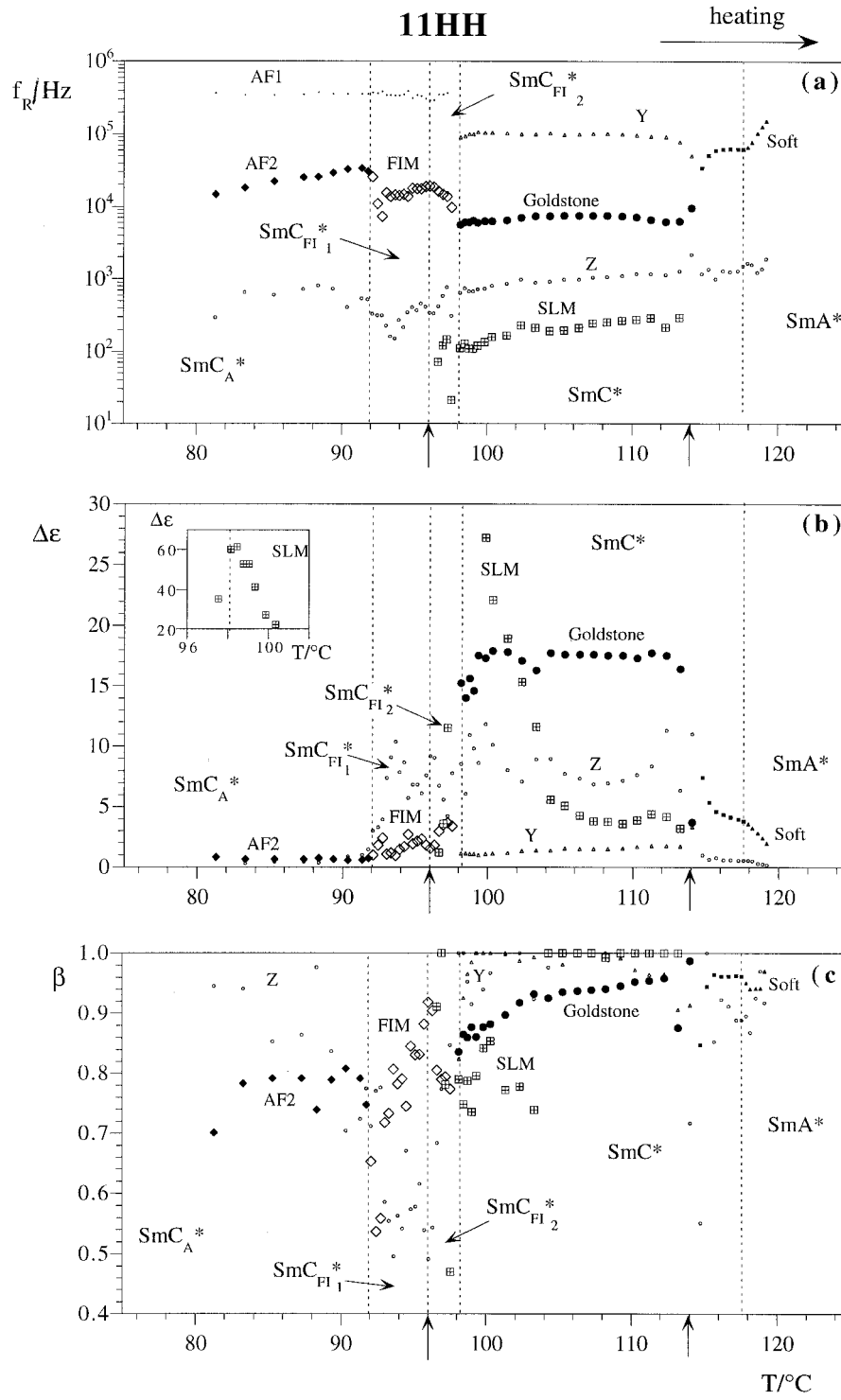

Figure 10. Relaxation frequencies (*a*), dielectric amplitudes (*b*) and dispersion parameters (*c*) of the relaxation modes detected for **11HH**, on heating.

The analysis of figures 14, 7, and 8 draws attention to an important correlation between the existence of disclination lines at zero field and the effect of the bias field on the dielectric constant. In the high temperature region of the SmC* phase, the dielectric constant decreases only for values of the bias field higher than ≈ 0.24 V μm^{-1}. In contrast, the dielectric constant in the SmC_{FI}^* phase and in the low temperature region of the SmC* phase decreases significantly with low bias field. These results reflect the reduced mobility of disclination

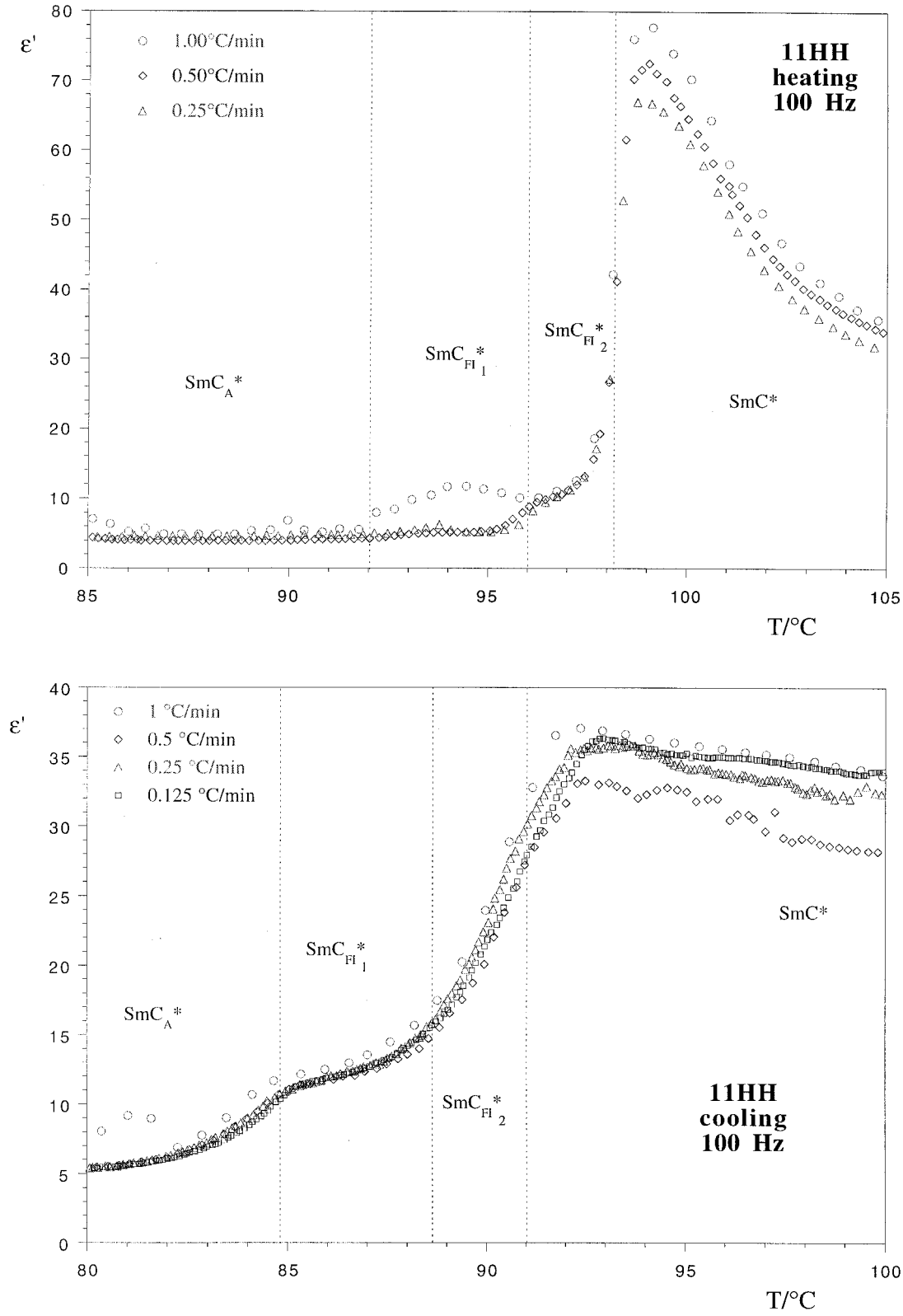

Figure 11. The real part of the dielectric constant, obtained at 100 Hz for **11HH**, at different cooling/heating rates.

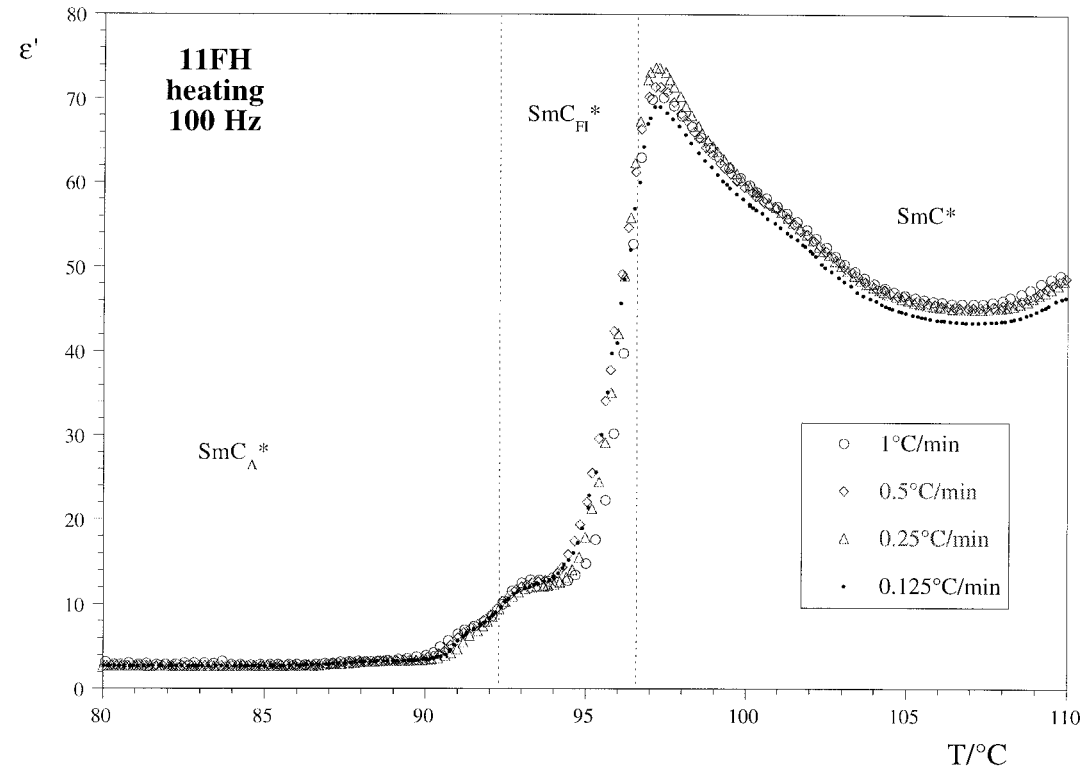

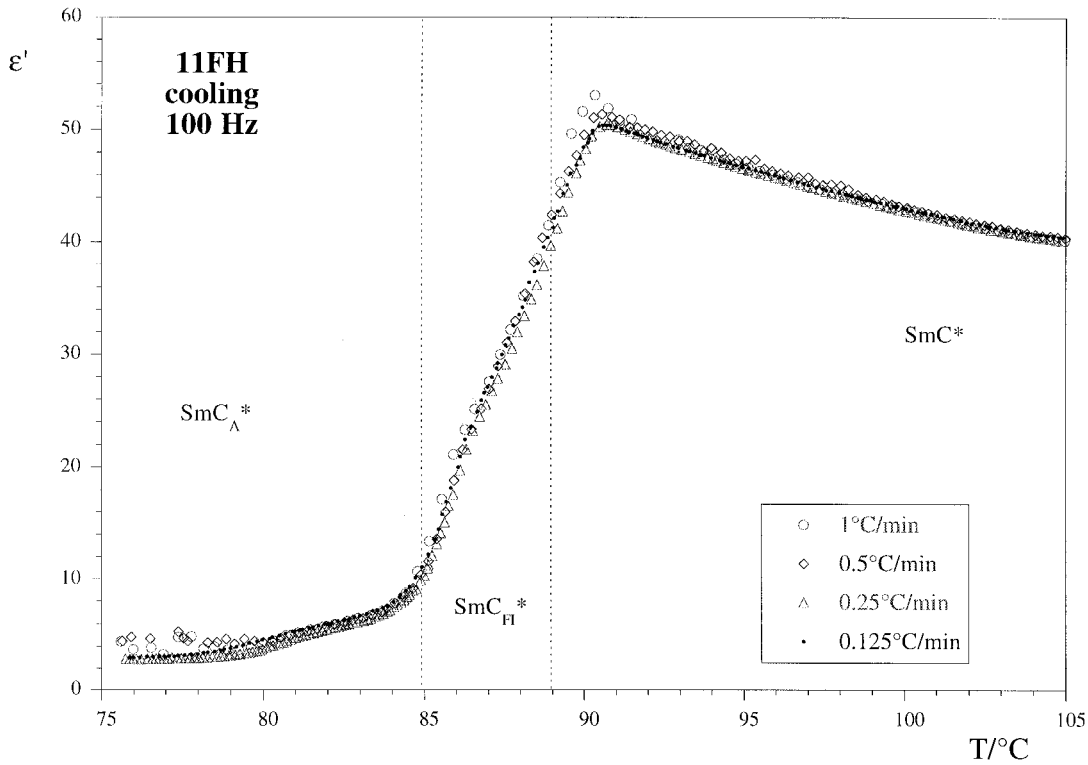

Figure 12. The real part of the dielectric constant, obtained at 100 Hz for **11FH**, at different cooling/heating rates.

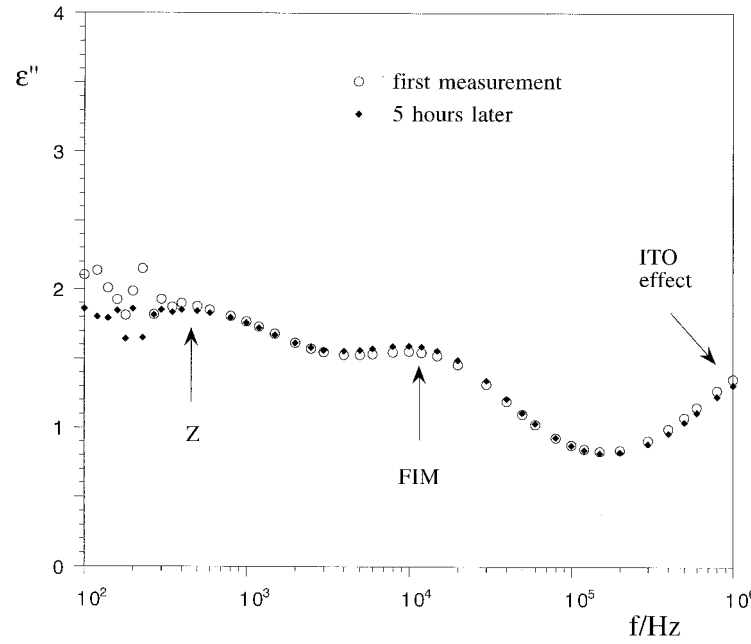

Figure 13. Dielectric dispersion data obtained in the $SmC^*_{FI_1}$ phase of **11HH**, at the stabilized temperature of 95.3°C, after heating the sample. The open circles correspond to a first measurement. After ≈5 h of repeated measurements, the second curve (full diamonds) was obtained.

lines under the bias field and the freezing of the helix in a partially unwound state, which reduces the contribution of both the SLM and the Goldstone mode.

We do not observe an increase in the dielectric constant at high temperatures when the bias field is high enough for disclination lines to appear. As the action of the bias field is to reduce the mobility of all charges and dipoles in the sample, it may be that the appearance of a small increase of the contribution from the SLM is masked by a decrease in the dielectric amplitude of the Goldstone mode.

3.6. *Summary of experimental results*

For the three compounds studied, **10FH**, **11FH** and **11HH**, we have obtained the following common results, apparently related to the SmC^*_{FI} phases:

(1) The electro-optic behaviour of all the SmC^*_{FI} phases studied is typical of ferrielectric-like phases.
(2) The dielectric relaxation spectrum obtained at stabilized temperatures in SmC^*_{FI} phases is stable over large periods of time.
(3) In the temperature interval of the SmC^*_{FI} phases and the neighbouring region of the SmC* phase, disclination lines (corresponding to 2π-disclinations) become visible by polarizing optical microscopy. One can say that: (a) the density of lines is always much higher on heating runs; (b) whenever these lines are visible, the SLM described by Bourny *et al.* [1] is detected; (c) the dielectric amplitude of the SLM is found to be related to the density of the observed lines; (d) the dielectric constant measured on cooling or heating runs usually presents a step in the temperature interval of the SmC^*_{FI} phases—this anomaly is apparently related to the contribution of the SLM.
(4) Two relaxation modes are repeatedly observed in SmC^*_{FI} phases: the SLM and the FIM. A high frequency mode, AF1, was also observed, but could not be characterized adequately.
(5) All the relaxation processes in SmC^*_{FI} phases are highly polydispersive.
(6) The FIM presents a low dielectric amplitude and its relaxation frequency is always lower on cooling than on heating runs.
(7) Although the contribution of the SLM depends on heating/cooling rates and the history of the sample, the temperature interval where SmC^*_{FI} phases occur is apparently independent of these parameters.

4. Conclusion

It is clear that, in order to describe theoretically the structure of SmC^*_{FI} phases, one must find a model that interprets consistently not only X-ray measurements [2], but also optical rotatory power, conoscopic results [5] and Raman measurements [16]. Dielectric spectroscopy, although not as powerful a tool as X-rays to probe the structure of liquid crystalline phases, can nevertheless reveal some important details. In the ferrielectric region of the three compounds studied, we have consistently found a weak FIM. This mode is probably

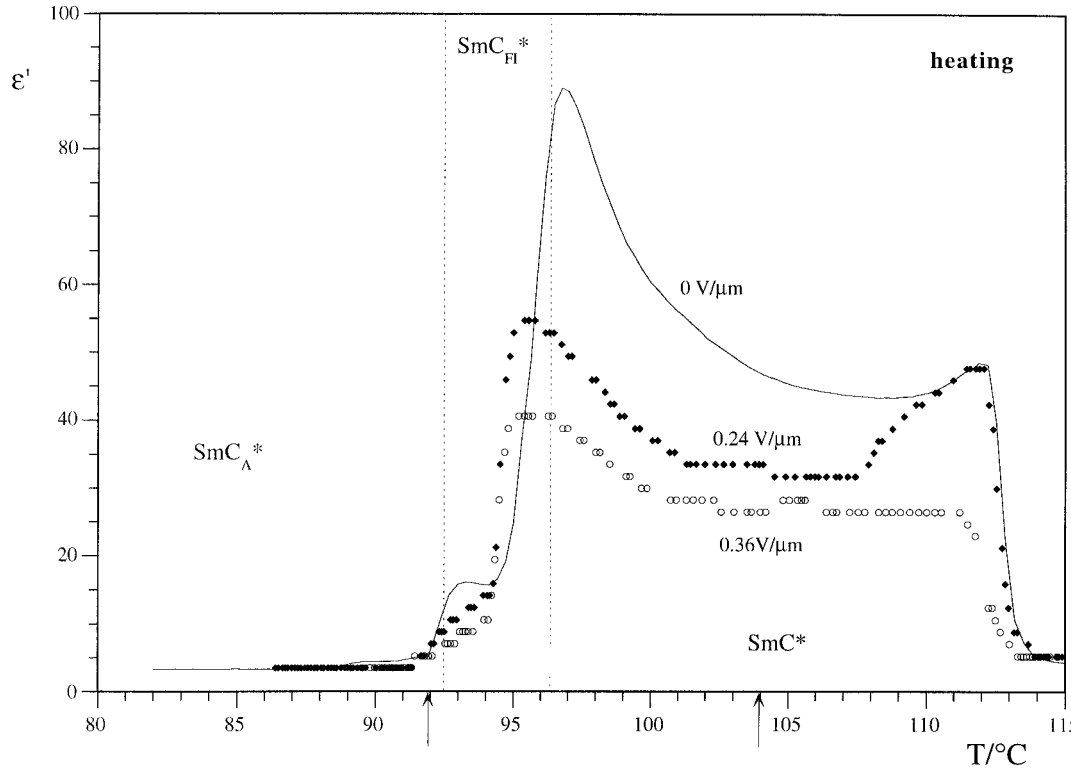

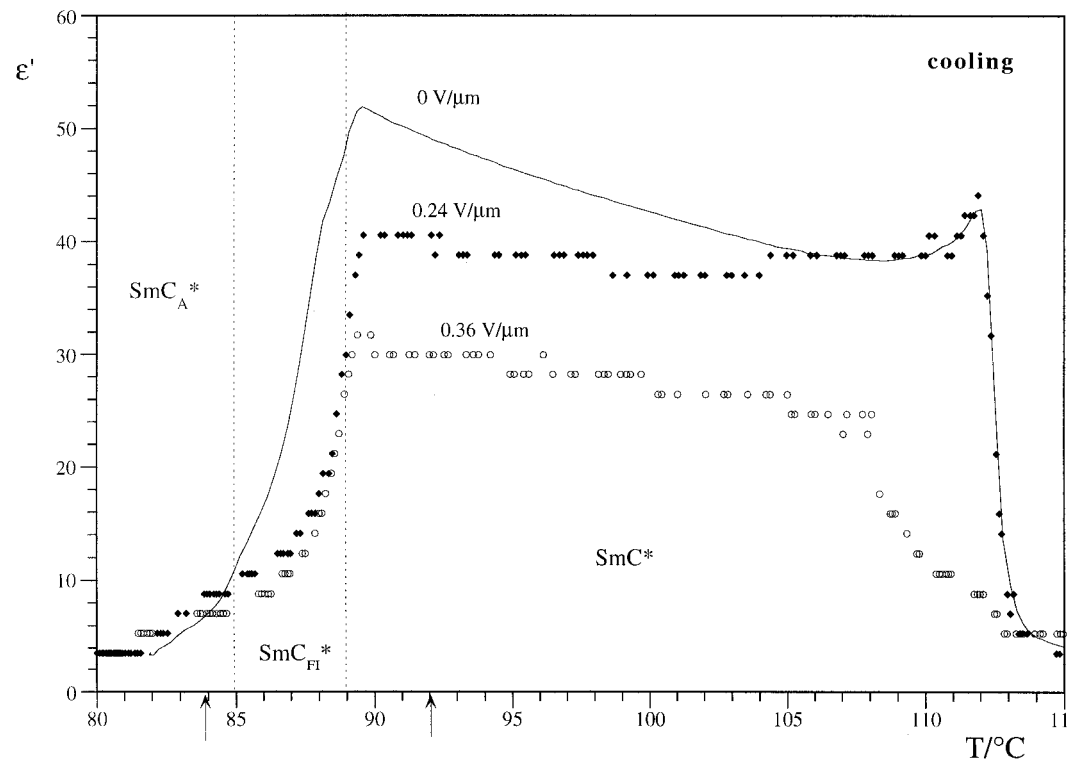

Figure 14. Real part of the dielectric constant, measured at 100 Hz as a function of the bias electric field, on cooling and heating runs, for **11FH**.

related to some azimuthal movement of the molecules. Moreover, it combines some characteristics similar to those of the Goldstone mode of the SmC* phase with certain features of the AF2 mode of the SmC^*_A phase. The resemblance to the Goldstone mode is more pronounced in the high temperature range of stability of the SmC^*_{FI} phase, albeit the similarity to AF2 is more explicit in the lower temperature range of stability of this phase. The relaxation frequency of the FIM is higher on heating than on cooling, probably reflecting some memory effect related to the physical properties of the previous phase.

The ferrielectric region was found to be highly stable, but to present highly polydispersive relaxation modes. The large number of defects usually presented by SmC^*_{FI} phases is certainly one of the factors that contribute to this polydispersivity, but other causes may also exist, such as a non-Cole–Cole relaxation behaviour or a non-linear coupling between modes, which have not been considered in our analysis.

Defects such as 2π-disclinations give an important contribution to the dielectric constant. We have found that the dielectric constant in SmC^*_{FI} and SmC* phases is very sensitive to bias fields, especially when 2π-defects are present. This feature, which is not observed in the SmC^*_A phase, may be of particular importance to the interpretation of what SmC^*_{FI} phases are, in terms of their structure and competitive interactions.

The authors are grateful to Dr M. Glogarová for helpful discussions and to Albano Costa for his technical assistance. This work was supported by the project PRAXIS XXI/3/3.1/MMA/1769/95. S. Sarmento and F. Pinto thank project Praxis XXI for the grants BD/9545/96 and BIC J/4688/96.

References

[1] Bourny, V., Pavel, J., Gisse, P., and Nguyen, H. T., 2000, *Ferroelectrics*, **241,** 247.

[2] Mach, P., Pindak, R., Levelut, A.-M., Barois, P., Nguyen, H. T., Huang, C. C., and Furenlid, L., 1998, *Phys. Rev. Lett.*, **81,** 1015.

[3] Čepič, M., and Žekš, B., 1995, *Mol. Cryst. liq. Cryst.*, **263,** 61.

[4] Čepič, M., and Žekš, B., 1999, oral communication in the 7th International Conference on Ferroelectric Liquid Crystals (FLC99), Darmstadt, Germany.

[5] Akizuki, T., Miyachi, K., Takanishi, Y., Ishikawa, K., Takezoe, H., and Fukuda, A., 1999, *Jpn. J. appl. Phys.*, **38,** 265.

[6] Isozaki, T., Fujikawa, T., Takezoe, H., Fukuda, A., Hagiwara, T., Suzuki, Y., and Kawamura, I., 1993, *Phys. Rev. B*, **48,** 13 439.

[7] Cluzeau, P., Gisse, P., Ravaine, V., Levelut, A.-M., Barois, P., Huang, C. C., Rieutord, F., and Nguyen, H. T., 2000, *Ferroelectrics*, **244,** 1.

[8] Buyvidas, M., Gouda, F., Lagerwall, S. T., and Stebler, B., 1995, *Liq. Cryst.*, **18,** 879.

[9] Hiraoka, K., Takezoe, H., and Fukuda, A., 1993, *Ferroelectrics*, **147,** 13.

[10] Moritake, H., Uchiyama, Y., Myojin, K., Ozaki, M., and Yoshino, K., 1993, *Ferroelectrics*, **147,** 53.

[11] Hou, J., Schacht, J., Gießelmann, F., and Zugenmaier, P., 1997, *Liq. Cryst.*, **22,** 409.

[12] Panarin, Y. P., Kalinovskaya, O., and Vij, J. K., 1998, *Liq. Cryst.*, **25,** 241.

[13] Fukui, M., Orihara, H., Suzuki, A., Ishibashi, Y., Yamada, Y., Yamamoto, N., Mori, K., Nakamura, K., Suzuki, Y., and Kawamura, I., 1990, *Jpn. J. appl. Phys.*, **29,** L329.

[14] Uehara, H., Hanakai, Y., Hatano, J., Saito, S., and Murashiro, K., 1995, *Jap. J. appl. Phys.*, **34,** 5424.

[15] Faye, V., Rouillon, J. C., Destrade, C., and Nguyen, H. T., 1995, *Liq. Cryst.*, **19,** 47.

[16] Yuzyuk, Y., Sarmento, S., Simeão Carvalho, P., Almeida, A., Pinto, F., Chaves, M. R., and Nguyen, H. T., 1999, *Liq. Cryst.*, **26,** 1805.

[17] Gouda, F., Skarp, K., and Lagerwall, S. T., 1991, *Ferroelectrics*, **113,** 165.

[18] Simeão Carvalho, P., Chaves, M. R., Destrade, C., Nguyen, H. T., and Glogarovà, M., 1996, *Liq. Cryst.*, **21,** 31.

[19] Carlsson, T., Žekš, B., Filipič, C., and Levštik, A., 1990, *Phys. Rev. A*, **42,** 877.

[20] Laux, V., Isaert, N., Nguyen, H. T., Cluzeau, P., and Destrade, C., 1996, *Ferroelectrics*, **179,** 25.

[21] Sarmento, S., Simeão Carvalho, P., Chaves, M. R., Nguyen, H. T., and Pinto, F., 1999, *Mol. Cryst. liq. Cryst.*, **328,** 457.

[22] Pavel, J., Gisse, P., Nguyen, H. T., and Martinot-Lagarde, P., 1995, *J. Phys. II (Fr.)*, **5,** 355.

[23] Sarmento, S., Simeão Carvalho, P., Chaves, M. R., Pinto, F., and Nguyen, H. T., *Liq. Cryst.* (submitted).

[24] Simeão Carvalho, P., Glogarovà, M., Chaves, M. R., Destrade, C., and Nguyen, H. T., 1996, *Liq. Cryst.*, **21,** 115.

[25] Simeão Carvalho, P., Glogarovà, M., Chaves, M. R., Nguyen, H. T., Destrade, C., Rouillon, J. C., Sarmento, S., and Ribeiro, M. J., 1996, *Liq. Cryst.*, **21,** 511.

[26] Žekš, B., 1999, tutorial in the 7th International Conference on Ferroelectric Liquid Crystals (FLC99), Darmstadt, Germany.